ARCHITECTURE CIVIL ENGINEERING ENVIRONMENT
The Silesian University of Technology
No. 1/2025

doi: 10.2478/ACEE-2025-0008

DESIGN CONCEPT OF VARIABLE, FLAT CUT BENDING-ACTIVE SHELLS

Armin FATHOLLAHI [a*], Valentina BEATINI [b]

[a] Graduate MSc student at Tabriz Islamic art university Department of Architecture, Iran
*E-mail address: *a.fatholahi96@gmail.com*

[b] Department of Civil and Architectural Engineering, Aarhus University, Denmark

Received: 4.07.2024; Revised: 1.03.2025; Accepted: 5.03.2025

Abstract

Bending active structures offer an efficient and sustainable way to form freeform shells by elastically deforming initially flat or linear elements. However, widespread adoption remains limited by the difficulty of reconciling structural demands, architectural requirements, and material constraints early in the design process. This paper proposes an integrated concept-design method that uses strategically placed cut-out patterns on a flat panel to combine linear ribs and thin plate elements in a single piece. A comparative study using Finite Element Analysis examines the performance of the proposed design when fabricated in plywood versus 3D-printed natural fiber-reinforced polymers. The analysis indicates that plywood, with its well-established fabrication methods and environmental profile, offers a practical solution under current conditions, whereas 3D-printed natural fiber-reinforced polymers present promising avenues for customization and material efficiency – albeit with a need for further validation of their processing parameters. By mapping the interplay between geometry, material selection, and manufacturing methods, the study underscores how early-stage design decisions can influence structural behaviour and overall environmental footprint, paving the way for future prototyping in sustainable architecture.

Keywords: **Curvature lines; Variable – mass material; Bending-active gridshells; Cut-out pattern; Design pre-rationalization.**

1. INTRODUCTION

Sustainable engineering design promotes a holistic approach that encompasses the entire lifecycle of structural systems. This approach becomes even more effective when integrated with innovative structures that maximize efficiency and constructability. According to Engel (Engel H., 1968), structures can be categorized based on how they carry loads – such as form-active, vector-active, and section-active systems – each with distinct mechanical behaviours and load-transfer mechanisms. Bending active structures, such as the renowned Mannheim Multihalle (1975), exemplify innovations within this framework. In these structures, initially straight or planar elements, bending deformation is intentionally induced through a form-finding process (Lienhard & Knippers, 2014). This induced deformation is replicated during the erection process, acting as a self-forming technique. Although bending-active structures are celebrated for their innovative and efficient use of materials, they remain underutilized in contemporary architectural design. This situation prompts an exploration into the barriers preventing their widespread adoption. Sustainability in architecture shall reverberate into structural, architectural and construction design decisions(Højbjerg et al., 2020). While existing methods for bending-active form-finding focus primarily on geometry and structural analyses, few approaches explicitly embed sustainability criteria into the earliest design stages. The integrated design of bending-active structures is challenging because it relies on complex analyses not readily accessible to all designers. These strategies must account for the nonlinear nature of the deformation process, monitoring residual stresses and their effect on structural stiffness. The core problem addressed in

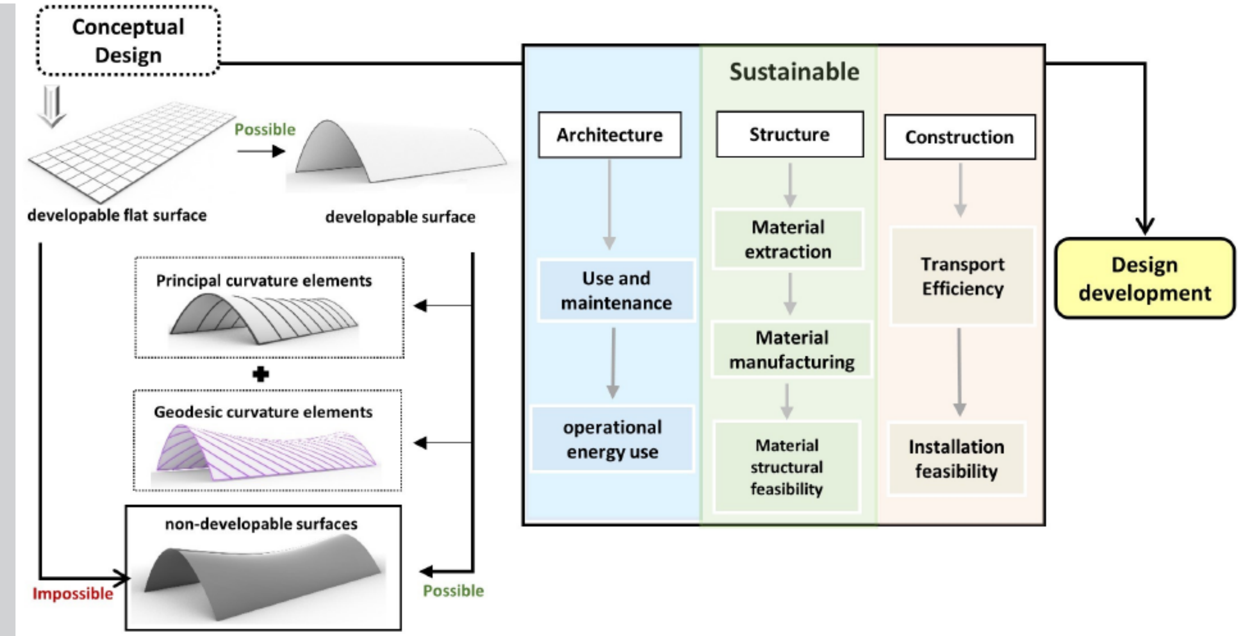

Figure 1.
Schematic of the structural concept design, and proposed aspects to be consider in the concept design of sustainable bending active structures

this paper is the lack of an integrated design approach from the earliest phases. Without integrated design strategies, structural, architectural, and sustainability considerations often remain isolated, leading to inefficient material usage and difficulties when integrating energy efficiency design solutions such as panels or surface elements.

Constructed applications of bending active structures are usually gridshells, where covering membranes are applied after bending linear elements. Bent plate elements may offer additional environmental advantages and have been explored by Buckminster Fuller (Buckminster, 1959), who famously questioned architects about the weight of their buildings, and, among others, in (Magna & Knippers, 2017). However, in these examples, plates are first bent and then interconnected, similar to standard gridshell structures (Højbjerg et al., 2020),which complicates the delivery process and requires custom joints.

As illustrated in Figure 1, left, according to Gauss's Theorema Egregium, a developable surface – originally flat – can only be transformed into another developable surface. In a previous study(Fathollahi & Beatini, 2024). a strategy was proposed to overcome the limitation by employing cut-out patterns. These, as exemplified by origami-inspired designs, enable the reproduction of non-developable surfaces composed rigid (Beatini, 2017) or flexible elements (Kansara et al., 2023; Zhang et al., 2015). The subtracted area is the area that would stretch or bend if present, allowing the surface to remain developable locally while transforming into a non-developable surface overall. This method enhances the structural and aesthetic versatility of bending-active structures and facilitates the creation of surfaces beyond developable ones. As schematized in Figure 1, the method includes simple geometrical considerations about the target surface's curvature, distributing principal and secondary elements on the originally flat surface to be fabricated. This refined approach supports early design explorations via simple physical models, enhancing accessibility for architects (Beatini & Royer-Carfagni, 2017).

To move toward implementation, it is necessary to evaluate how these architectural and structural possibilities relate to constructability and whether the solution meets environmental sustainability aspects, such as reduced material emissions and improved constructability. This paper aims to bridge the gap between the conceptual design of bending active structures using cut-out patterns and their real-world applications. Referring back to Figure 1 (right), it highlights the integrated role of design variables that affect sustainability – addressing not only geometry but also material suitability, construction technologies, and efficiency during usage. To achieve this, it conducts comparative technical analyses of possible construction technologies and suitable materials in

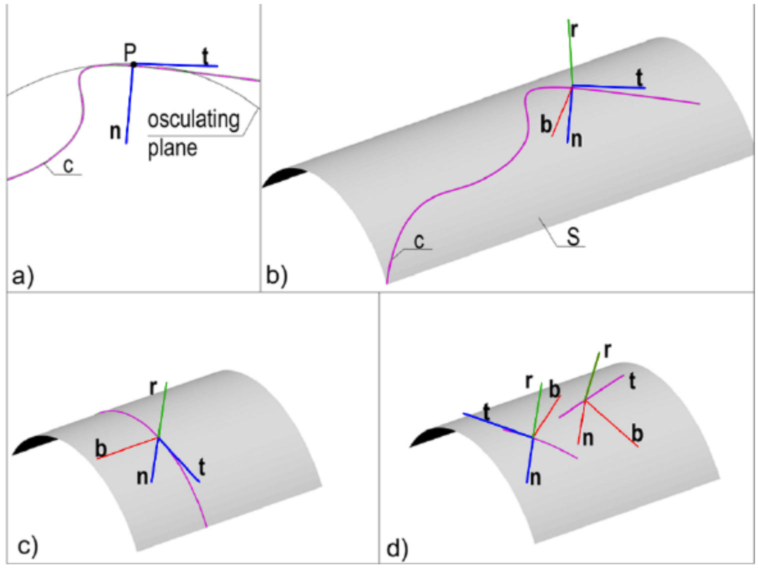

Figure 2.
Curvature of a curve on a surface. a) the curve and its curvature frame; b) the Darboux frame of a curve lying on a surface; c) a curve of zero geodesic torsion on a surface; d) a curve of zero geodesic curvature on a surface

terms of structural performance and environmental impact. Finally, the paper suggests 3D-printed Natural Fiber Reinforced Polymer (NFRP) and laser-cut plywood as candidate materials, and discusses the steps ahead toward implementation. his paper aims to bridge the gap between the conceptual design of bending-active structures using cut-out patterns and their real-world applications.

2. CONCEPT DESIGN

2.1. Geometry of curves on surfaces

The proposed concept, schematized in Figure 1, features a hierarchical system comprised of structural ribs that span between supports. The dimensions and orientation of these ribs, which align with principal curvature lines, are primarily dictated by structural requirements. Secondary elements, including surface elements, are shaped and sized to integrate architectural demands while adhering to geodesics traced between key points on the identified curves. The concept design necessitates knowledge of the orientation of the curve on surfaces. A generic curve $c \in R^3$, shown in Figure 3a, is described by its tangent ***t*** and normal *n* unit vectors. The latter, lying on its osculating plane, evaluates how much a point *P* moving along the curve changes direction over time. When the curve lies on a surface *S*, the relationship of the point with both the curve and the surface can be expressed using the Darboux frame, which consists of the tangent unit vector *t* to the curve, the normal unit vector *r* to the surface, and the binormal *b* to these vectors (O'Neill, 2006), Figure 3b. This frame is crucial in the bending active process as it computes not only the bending of the structural surface elements, but also their orientation on the surface. Specifically, three parameters are recognized: the normal curvature, k_n, the geodesic curvature, k_t, and the geodesic torsion, t_g. The latter measure how fast the osculating plane $(t \times n)$ is rotating around the tangent t. Curves whose normal *n* coincides with the surface normal *r* have zero geodesic torsion, $t_g = 0$, Figure 3c. These are the principal curvature lines. The geodesic curvature measures how fast the osculating plane $(t \times n)$ is rotating around the binormal vector *b*. A curve with zero geodesic curvature, $k_g = 0$, does not "steer" out of the surface's tangent plane, exhibiting no sideways curvature, as depicted in Figure 3d. At any point on a surface, two orthogonal families of principal curvature directions exist (infinite curves at umbilical points). Additionally, more geodesics can be traced from a given point, which vary according to the initial tangent or point they are directed towards (Radeschi, 2017). These two special classes of curves are always present on the surface and are used here to guide the concept design. Finally, the case of zero normal curvature, $k_n = 0$, gives rise to the so-called asymptotic curves, where the tangent plane of the surface and the osculating plane of the curve coincide. Here, straight elements can be used (Schling et al., 2022), but unfortunately not all surfaces include this kind of curves.

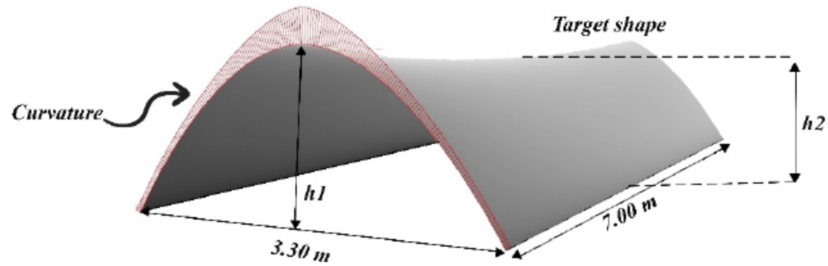

Figure 3.
Case study of a barrel shell with anticlastic surface and pointed arch cross section

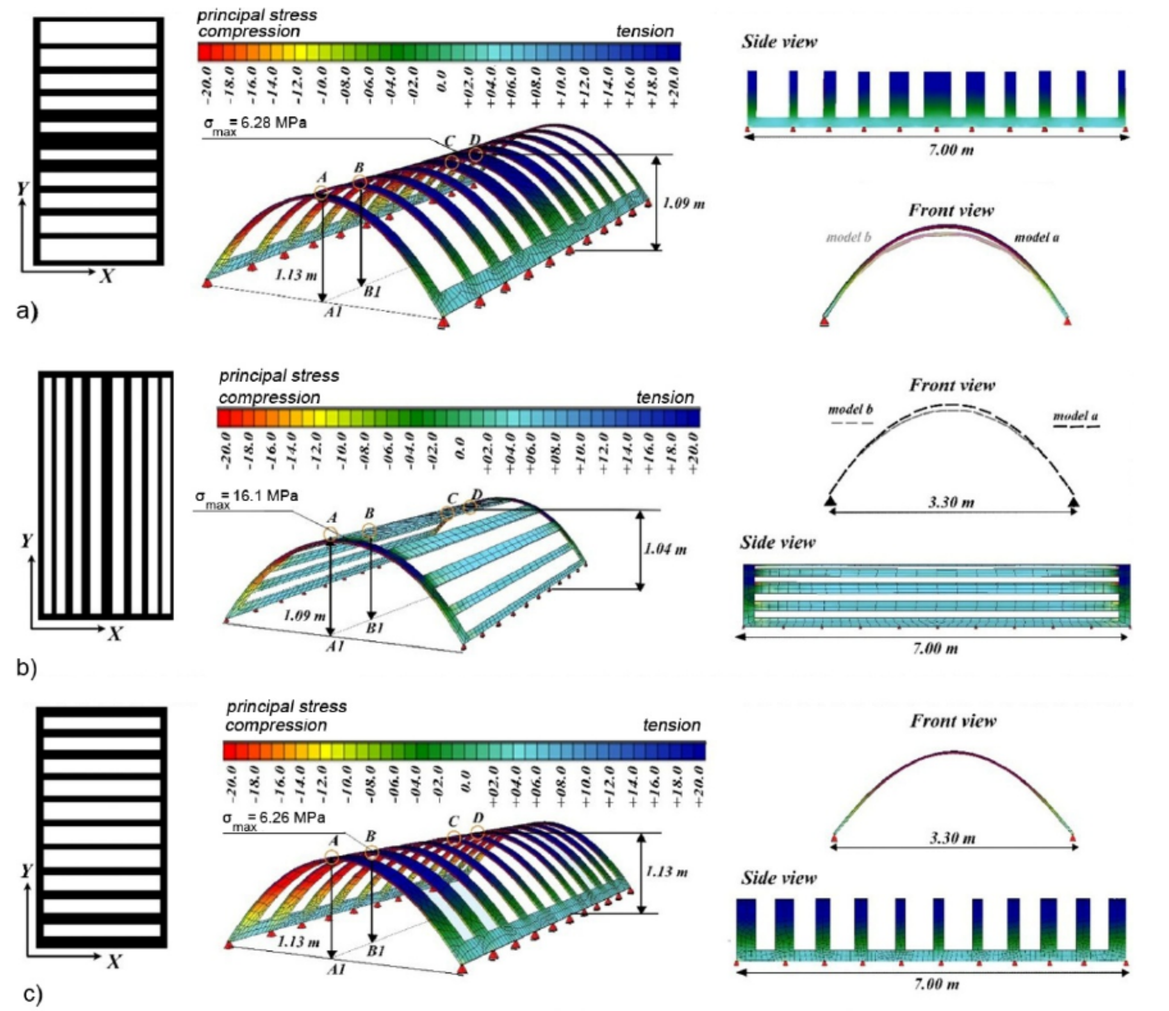

Figure 4.
Comparison between three bending active gridshells having the same bounding area but different designs. Considering the geometry moving from the edges of the structure to its centre: (a) a structure composed of transversal elements of progressively larger width; (b) a structure composed of longitudinal elements of progressively larger width; (c) a structure composed of transversal elements of progressively smaller width

2.2. Principal curvature elements

The initial step in the concept design process involves tracing principal curvature lines between supports. These lines, being paths of maximum curvature, act as paths of least resistance where uniformly distributed gravitational forces, such as self-weight, naturally tend to flow. By aligning elements along principal curvature lines, the design ensures that each element bends only along its longitudinal axis. The detailed design must ensure that sizing and spacing of the elements allow them to bend within the material's strength limits, as derivable from the bending moment formulation

$$f_{m,u} \geq \frac{1}{\rho_u}\frac{t}{2}E, \qquad (1)$$

where E is the modulus of elasticity, t is the thickness of the element, whereas ρ_u is the radius of curvature and $f_{m,u}$ is the allowable bending strength of the material, all in the given longitudinal direction u.

At the level of detail appropriate for a concept design, designers can consider that the local moment of inertia I_u, and thus the associated cross-section, will need to vary along the longitudinal direction u as a function of the target curvature $1/\rho_u$. This relationship is defined as

$$\frac{1}{\rho_u} = \frac{M_u}{E_u I_u}, \qquad (2)$$

where M_u is the applied bending moment. By modifying the moment of inertia between the ribs, it is possible to locally adjust the derived curvature. This principle can be utilized to explore alternative design concepts. Figure 4 illustrates a target surface, a barrel shell with a pointed arch cross section and negative Gaussian curvature, the latter indicated by a different height of the end and mid cross sections. Two gridshell structures are proposed to approximate it via bending active, Figure 4. Each model in its flat state covers an area A = 4.15 m x 7.00 m and has a thickness h = 30 mm. The models are designed assuming material parameters: E = 9.05 GPa, ultimate flexural strength $f_{m,u}$ = 120 MPa, and density d = 1200 kg/m^3. These parameters are representative of the average material proprieties of Natural Fiber Reinforced Polymers (NFRP) (Wang et al., 2022) (Gengnagel et al., 2013). As discussed in Section 3, this material can be further manipulated for substantial deformations at the cost of lowered material's strength capabilities.

The geometry of the models varies: one is a gridshell characterized by transversal elements of progressively larger width the closer they are to the central transversal axis (Figure 4a); the second one is a gridshell characterized by longitudinal elements of progressively larger width the closer they are to the longitudinal mid-axis (Figure 4b). The third design features a gridshell with transversal strips that are widen towards the edges (Figure 4c). The gridshells have been modelled as shell elements in Finite Element Analysis (FEA), assuming large deformations, which allows us to account for the variation in load and stiffness due to deformation and axial internal forces (Lázaro et al., 2017). The simulation follows a stepwise approach. Initially, a vertical force of 0.5 kN/m is applied along their longitudinal axis, followed by its removal and a progressive displacement of a total of 0.6 m along one longitudinal edge, until the structure reaches a transversal span of 3.30 m. The results of the deformation process, visualized in 3D, front, and lateral views (principal stress, located in the middle of the wider element, reaches +6.28 N/mm^2). The composed model clearly shows an anticlastic curved form. The mid elements bend less due to their larger moment of inertia. Structurally, each transversal element acts relatively independently; since all transversal elements share the same boundary conditions, their principal stress at the end of the bending process has a similar distribution. This design aligns with the strategy highlighted in Section 2.1. The model with longitudinal elements progressively larger (Figure 4b) reaches a l span of 3.31 m and shows an increased sag of c.a. 5 cm. The height of the deformed model along the longitudinal length at points A, B, C, and D in the figure is 1.09m, 1.08m, 1.05m, and 1.04m, respectively. The longitudinal elements are not directly involved in bending; they act as beams carried by the end arches. This indicates that the sag of the longitudinal elements is mainly due to deformation at their joints and length. Compared to the previous example, this design comes along substantially increased stress, up to +16.1N/mm^2; moreover, the stress distribution is non-uniform, and there are notable stress concentrations at the joints, which impact the structural integrity and complicate the construction process. The model with transverse elements gradually widening towards the edges (see Figure 4c), has nil or negligible sag, the model's shape resembles a barrel shell. While the stress distribution resembles the case in Figure 4a, locating the thinner, more flexible elements toward the middle of the structure counteract the possibility to have a significant sag. These examples illustrate the interrelation of structural, formal, and construction decisions. Whether there are alternative strategies to achieve the barrel shell profile, relying on the principal curvature lines for a uniform distribution of the main structural elements spanning between supports is a structurally sound approach that allows design alterations (here, the longitudinal sag).

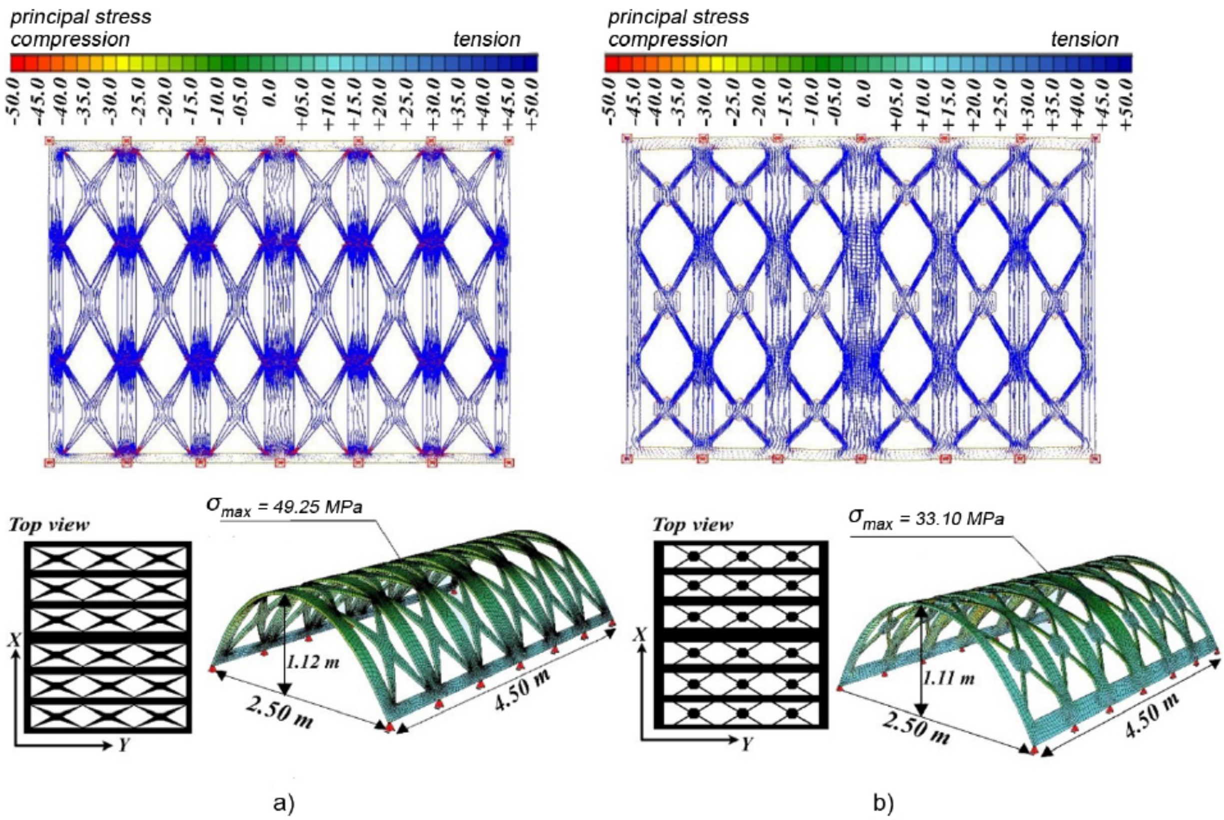

Figure 5.
Comparison of two bending active gridshells in the erection process, composed of the same main elements but having secondary elements of smoothly variable width (a) and of discontinuous width (b). Map of the principal stress (above), originally flat surface (bottom left) and deform

2.3. Secondary Geodesic design elements

The second step in the design process involves adding secondary elements to enhance the stiffness of the primary elements, countering potential buckling from eccentric loads or excessive slenderness. Additionally, surface elements may be incorporated to modulate sunlight, create desired visual patterns, or provide more substantial support for covering materials, thus simplifying their connections. All these elements can be oriented in geodesic directions to ensure they conform to the surface without warping. Despite this strategic orientation, as demonstrated in the previous example, the varying curvature of elements at their intersection points can still induce undesirable stress concentrations due to torsional deformation. In (Tellier et al., 2021), a method is described for constructing gridshells with minimal torsional stress by aligning elements along geodesic lines. At the opposite, one might accept some level of torsional stress as a structural compromise to explore the architectural appeal of deformed, twisted ribs, as discussed in (Khojastehmehr & Filz, 2023). The approach proposed here sits in the middle and aims to balance structural integrity with aesthetic goals. For the intended shape, the design seeks to leverage the geometrical stiffness of the elements to achieve the required twisting without incurring excessive torsional stress. This could allow to design elements to resemble specific motifs and culturally resonate, a theme widely explored by designers (Beatini, 2017a) (de Grey, 2000).

Figure 5 illustrates two structural surfaces employing main structural ribs, oriented along the direction of principal curvature, and secondary thinner elements oriented along geodesic lines. The structures are made by the same material earlier described and differ in such in case a, (Figure 5a) the geodesic elements have variable thickness, whereas in case b, (Figure 5b) large elements oriented along geodesic lines are connected to the main ribs through thin, secondary elements, acting as hinges. The resultant principal stresses in the two structures are in the ration a/b = 1/7. Design (a) results in high stress throughout the surface, with peaks at the intersection areas; in design (b), the stress is lower throughout and added surface elements are areas of minimal stress (in absolute values) within the structural surface. The differences can be explained considering how torsion deformation interacts with the cross section.

Consider two surface elements, Figure 7, rigidly interconnected, one having width b_1 and one having width $b_2 = \frac{b_1}{10}$, subjected to a uniform torsion T at supports. For given modulus of rigidity G of the material, and cross section proprieties ($\alpha b t^3$), where α is an approximation coefficient (Young et al., 2002), the applied torsion is related to the gradient of twist $\frac{d\theta_2}{dl_2}$ according to

$$T = G\ \alpha_1 b_1 t^3 \frac{d\theta_1}{dL_1} = G\ \alpha_2 b_2 t^3 \frac{d\theta_2}{dL_2}, \tag{3}$$

which leads to

$$\alpha_1 b_1 \frac{d\theta_1}{dL_1} = \alpha_2 b_2 \frac{d\theta_2}{dL_2}. \tag{4}$$

For b_1=10t, and b_2=t, this results in

$$\frac{d\theta_1}{dL_1} = 0.045\ \frac{d\theta_2}{dL_2}. \tag{5}$$

Therefore, deformations concentrate on the thinner section.

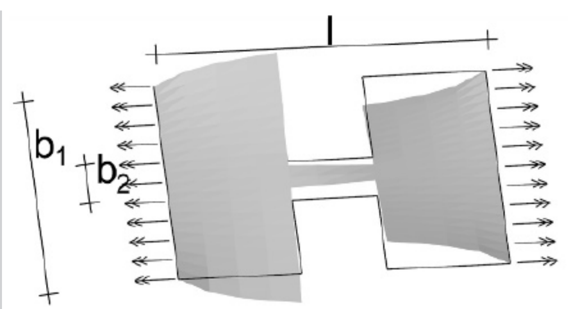

Figure 6.
Torsion deformation of a plate of variable width

Considering these observations, the fabrication process of the cut-out pattern shall allow the insertion of relatively thin, slender elements to lower the torsional stress, and maximize the architectural freedom in shaping the surface elements.

3. SUSTAINABILITY

3.1. Sustainability criteria

For the architectural, structural and construction characteristics and constraints outlined in the previous chapters, this section evaluates the sustainability implications of the proposed bending active structures. European regulations mandate that sustainability analyses should cover the entire lifecycle of a building. Table 1 summarizes the significant aspects discussed within each phase identified by EN 15978 and EN 15804 standards.

Table 1.
Significant factors characterizing active bending systems in each phase

Product	(A1–A3)	A1- A2 Material extraction and transportation
		A3 Manufacturing
Construction process	(A4–A5)	A4: Transport to the building site
		A5: Installation into the building
Use	(B1–B7)	B3 Repair
		B6. Operational energy use
End of Life	(C1–C4)	C4. Disposal
After use	(D1-D4)	D: Reuse, recovery and/or recycling potentials

3.2. Product stage

3.2.1 Material extraction

As mentioned in Section 2.1, not all materials are ideal for bending active structures. Suitable materials are those with a high ratio R of flexural strength to elastic modulus, allowing for significant deformations during shaping, while retaining enough residual strength to support loads (Lienhard, 2014). NFRP, simulated in previous sections, exhibits ratios from 10 to 50 MPa/GPa, depending on matrix composition and processing method (Kotelnikova-Weiler et al., 2013). Based on similar considerations, in (Douthe et al., 2010), a qualitative comparison of materials led to the choice of GFRP for durable bending active structures, and its sensitivity to long term effects was tested.

Table 2 contrasts this ratio and other properties with other materials like GFRP, timber, plywood, and bamboo, which, despite their lower customization potential, are also used in bending active gridshell or alternative, traditional free form gridshells. The previous observations are here integrated with data on the environmental footprint, measured using the carbon factor (CO2e per kg), excluding carbon storage. This value specifically addresses the carbon dioxide emissions which are directly related to climate change. According to the Embodied Carbon Database, timber has the lowest carbon factor

Table 2.
Material Properties and Environmental Impact

Material	Flexural Strength/Modulus Ratio (MPa/GPa)	Manufacturing Techniques	Embodied Carbon ($kgCO_2e/kg$)	Already employed in Bending-active Structures	Density (kg/m^3)
NFRP	10-50	3D Printing, CNC Drilling	Variable; lower than GFRP	Yes – furniture scale	800 to 1500
Plywood	4-11.13	CNC Cutting, Molding	1.07	yes	500-800
Glulam	2.07-2.45	Lamination CNC	0.512	yes	400-700
Timber, bamboo	1-11	Cutting, Shaping	0.493	yes	400-700
GFRP	10-12.5	CNC Cutting	2.63 to 6.72	yes	1800 to 2100

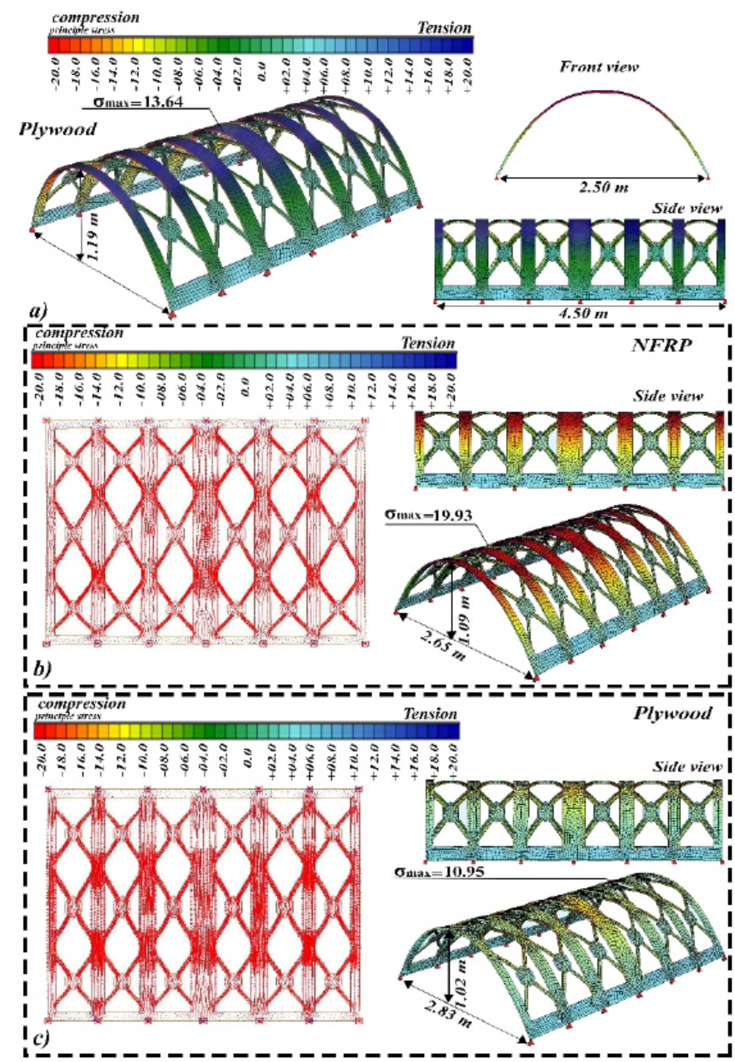

Figure 7.
(a) Active bending gridshell in the erection process when constructed in plywood made with the same design (b) Active bending gridshell made of NFRP under a uniform distributed gravity load (c) gridshell system created with plywood under a uniform distributed gravity load

(Table 2), followed by glulam and plywood, and detached, GFRP. The carbon factor of NFRP is difficult to set due to the specifics of the production process, however, it can be assumed that its natural fibre content and less energy-intensive production (15 to 45 MJ/kg versus 30 MJ/kg to 50 MJ/kg of

GFRP) make its carbon factor somehow lower than the one of GFRP.

3.2.2. Material manufacturing

Bending-active structures are highly material-efficient, minimizing waste by maximizing the structural capabilities of minimal resources. In contrast, the complexity of shaping glulam for traditional gridshells may lead to underestimated waste figures. The potential intricacy of patterns created by the design lends itself well to CNC laser cutting and 3D printing. Laser cutting and CNC technologies suit the layered nature of glulam and plywood. Despite being nascent, 3D printing for NFRP has begun implementation, enhancing façade elements, shell constructions (Tuli et al., 2024), and, notably, furniture designs that incorporate bending active (Saslawsky et al., 2024). 3D printing NFRP streamlines the production process by integrating fibre impregnation, deposition, and curing into one step, facilitating large-scale printing and customization through functionally graded materials (Kansara et al., 2023), potentially stiffening joints more effectively.

These observations suggest that plywood remains a competitive choice due to its sustainability credentials whereas NFRP offers significant environmental and mechanical benefits for bending active structures. These two options are therefore further considered in the successive analyses.

3.2.3. Material structural feasibility

To evaluate the technical feasibility of the two options, in Figure 7, the NFRP structure already in Figure 5 (b) is compared with the very same structure when constructed in plywood, assuming for this material a modulus of elasticity $E = 4.4$ GPa and ultimate flexural strength $f_m = 40$ MPa, such that $R = 9.09$. In the case of NFRP, it was $E = 9.05$ GPa, $f_{m,u} = 120$ MPa and $R = 13.25$. The plywood structure bends more, due to the lower modulus of elasticity, but the stresses in both options are well within the limits of the materials. and both materials will be considered in the successive design conceptualization phases.

3.3. Construction process stage

Bending active mitigates the logistic challenges associated with transporting large or non-easily packable curved elements typical of gridshells (Chilton & Tang, 2016). Additionally, the proposed system offers advantages over both standard and bending active gridshells. While nodes, intra modular joints, ground anchors, and lifting equipment are still required during the erection phase, the need for scaffolding and particularly joints is significantly reduced. If the process involves 3D printing, it may be feasible and preferable to print on-site to avoid potential damage during transportation.

However, the installation phase introduces more uncertainties. The selected materials have relatively low density (Table 1) and the installation strategies for bending active structures could be implemented.

These may involve pushing and deforming from below, or, where geometry permits, lifting the structure already deformed at the ground level (Quinn & Gengnagel, 2015). For smaller or simpler structures, lifting by cranes or using pneumatic formwork is possible (Naicu, 2012). Regardless of the method, numerous ground supports integrated with cables or shear connectors are needed to allow deformation, and precise movements are crucial to minimize the risk of overstressing the material during the erection process. The proposed design requires fewer parts to be moved; however, since the connections are already in place, this must be done with even greater care to avoid stress concentrations or unwanted deformations.

If made of plywood, the wood-based material used in gridshells typically involves moderate-strength timber products (not higher than European strength class C30 or D30), further necessitate that the bending process be carried out very slowly, usually over several weeks and with a very high moisture content in the laths to facilitate stress dissipation and prevent premature breakage (Harris et al., 2003) (Liuti et al., 2018). To better visualize the challenges related to the erection process, a timber model was constructed (Figure 8). The model's scale, 1:5, was chosen based on the minimal timber thickness available, which was 3 mm. The flat cut-out pattern was obtained by computer numerical control (CNC) machining (Figure 8a). Ad hoc elements were introduced to restrict the structure's transversal movement while permitting rotation. Fixing the structure in the longitudinal direction was unnecessary, and the structure exhibited no out-of-plane deformation (Figure 8c). The bending process was performed manually until the span and sag were comparable to those of the designs already tested in Figure 5 (see Figures 8d and 8f). The model has a structural span of 50 cm, a length of 140 cm, and a height of 23.4 cm. As discussed earlier, the process typically requires several weeks. Here, the timber was pretreated with hot water before

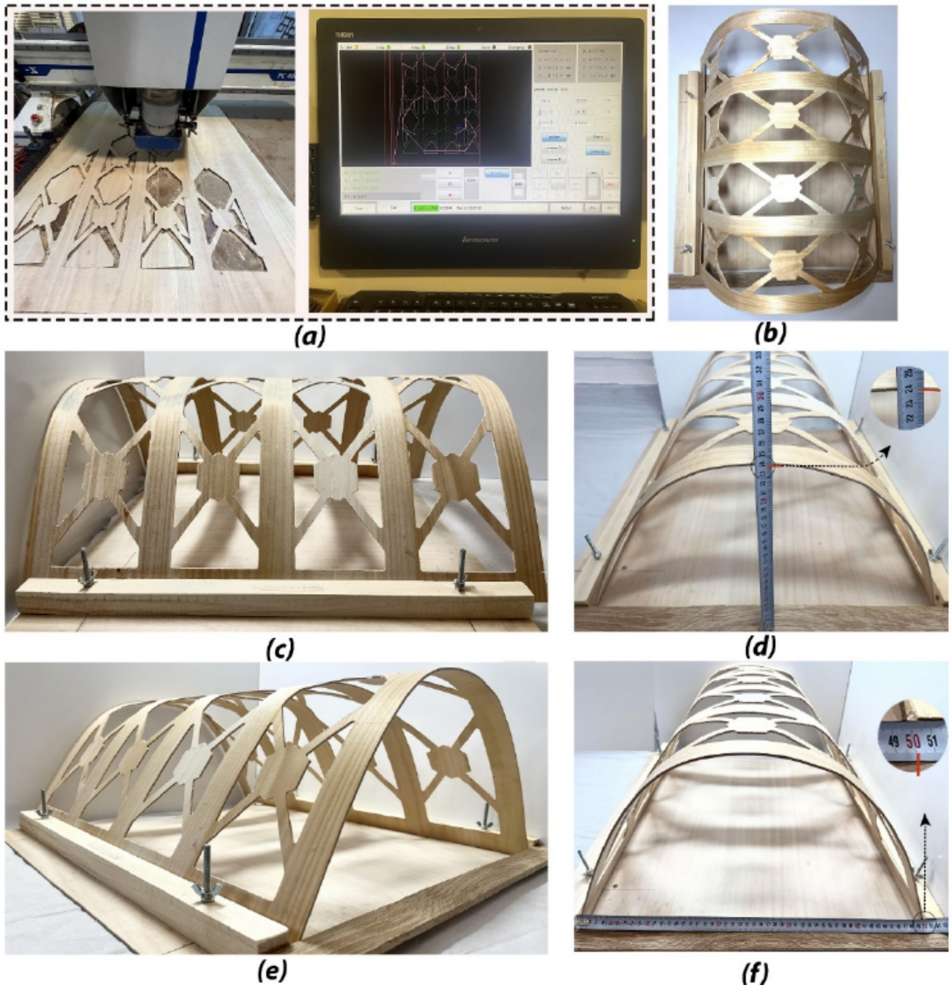

Figure 8.
A timber physical model was constructed at a 1:5 scale. (a) The CNC process utilized for the flat timber sheet, (b, c) the top view and side of the timber grid shell after the erection process, respectively, (d) The front view, highlighting the height in the middle of the span point (23.4 cm), (e) a perspective view of the timber model, and (f) the span of the model after the erection process measures 50 cm

bending, enabling the desired shape to be achieved within one prototyping session. Figure 8 also provides different views of the physical model in its final position, including top, side, front, and perspective views. No delamination or visually noticeable defects emerged.

3.4. Use stage

Live loads, especially horizontal ones like those caused by wind, can greatly affect the behaviour of lightweight structures. For barrel roofs, horizontal loads induced by wind are a major concern.The plywood gridshell was subjected to a uniform horizontal load $w = 0.5$ kN/m^2 acting along both longitudinal and transversal sides, with results depicted in Figure 9. Notably, wind loads along the transversal direction (Figure 9a) induce significantly higher stress levels compared to longitudinal loads (Figure 9b), indicating asymmetric stiffness. Resistance to the longitudinal load is indeed offered by the multiple arches and the stiffening action exerted by the secondary elements. The material distribution does not equally favour resistance along the transversal direction. This observation underscores the need for optimizing the shell's whole shape, for example increasing its anticlastic curvature, to enhance resistance where the chosen material distribution is insufficient.

Regarding energy efficiency, gridshells typically form part of a building's envelope and thus play a vital role in controlling energy flows. Bending active gridshells, however, are frequently used as temporary structures and are traditionally covered with PVC membranes that are heat-sealed or stapled after construction – an

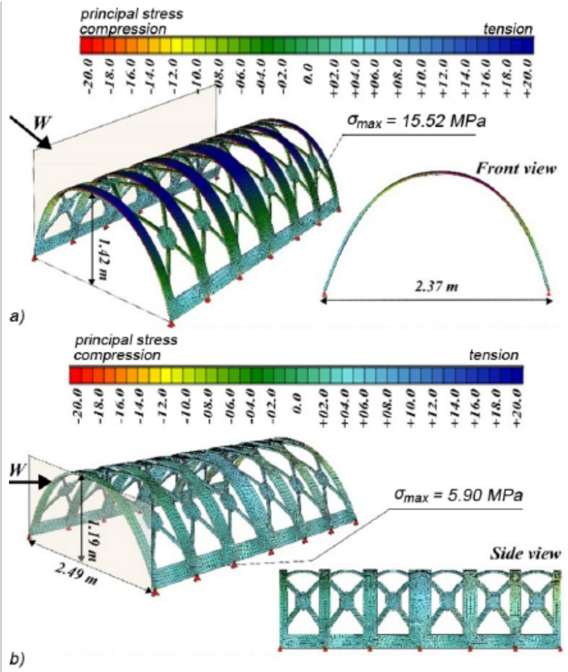

Figure 9.
Plywood grid shell under uniform horizontal loads, (a) uniform wind loads along the transversal direction, (b) uniform wind loads along the longitudinal loads

approach with limited environmental benefits.

By contrast, the proposed concept integrates opaque surface elements into the bending active structure from the outset, making it easier to anchor larger, flat supports for glass or other panels. Glass can improve environmental performance but demands tight dimensional tolerances (Douthe et al., 2017) and more robust load-carrying capacity.

To examine usage requirements further, two scenarios were evaluated. A temporary usage was modelled assuming that the structure is covered by a lightweight membrane of negligible weight. A uniform horizontal wind load $q_{h,t} = 0.5$ kN/m^2 was applied in the more critical (transversal) direction. The thickness of the structure was increased until the differential deflection – comparing the bent shape to the loaded shape – reached approximately 1/130. A prolonged usage scenario was modelled assuming that the structure was covered by glass panes, represented by a uniform vertical load of $q_v = 0.2$ kN/m^2. A higher uniform horizontal load $q_{h,p} = 1$ kN/m^2 was applied in the transversal direction. The structure's thickness was increased until deflection remains below 1/280. In both scenarios, it was ensured that the stresses did not exceed 35% of the allowable stress for NFRP or 50% of the allowable stress for plywood, in such allowing a larger safety factor for the NFRP structure due to manufacturing uncertainties. Results from the simulations are reported in Table 4.

Under these conditions, the temporary scenario for plywood required a thickness of 4.85 cm, whereas the longer-term scenario (with glass) required 5.59 cm. For NFRP, the corresponding thicknesses were respectively 4.05 cm and 4.60 cm, suggesting that NFRP's higher allowable stress capacity may make it more suitable for long-term usage with heavier or more demanding coverings. Moreover, NFRP is known to be sensitive to humidity (Oun et al., 2024), and the lack of discrete joints in the proposed system may make any required repairs more complicated. Therefore, a continuous, durable covering may well suit the challenges of the material. Proceeding in this direction, it would be necessary to study careful connection detailing to minimize repair needs. This is confirmed by (Liuti et al., 2018), where a comparative study of 24 bending active case studies showed that comprehensive design of details can offer significant economic advantages for larger or permanent projects.

Table 3.
Results of the simulation of temporary and prolonged usage for the design already in Figures 7 and 9, made in plywood and NFRP

Scenario	Plywood	NFRP
Temporary usage $q_{h,t} = 0.5$ kN/m^2	$\frac{\Delta_{bent}}{\Delta_{loaded}} = 1/125$ t = 4.85 cm	$\frac{\Delta_{bent}}{\Delta_{loaded}} = 1/131$ t = 4.05 cm
Prolonged usage $q_v = 0.5$ kN/m^2 $q_{h,p} = 0.5$ kN/m^2	$\frac{\Delta_{bent}}{\Delta_{loaded}} = 1/277$ t = 5.60 cm	$\frac{\Delta_{bent}}{\Delta_{loaded}} = 1/277$ t = 4.60 cm

3.5. Disposal and after use stages

Recycling practices, including reuse, repurposing, and material or energy recovery, can be complicated by contaminants such as screws and other hardware. Cut-out bending active structures, appear a profitable for recycling compared to traditional gridshells due to the fewer joints. Table 4 illustrates alternative materials used in bending active in relationship to end of life available processes and options. As one may expect, wood offers the most extensive recycling opportunities, available by relatively cheap mechanical processes. The presence of adhesives in products like glulam complicates mechanical recycling and energy recovery, as adhesives may impede the separation of layers. Mechanical recycling of GFRP can led to decreased mechanical properties and such loss of value (Wei & Hadigheh, 2022) (Chauhan et al., 2022), whereas the most effective thermal or

Table 4.
End of life options

Material	Methods	Options	Cost	Barries	Markets drivers
NFRP	Mechanical	Recover	Low	Degraded mech. proprieties	Automotive industry, consumer goods, energy production
	Thermal	Repurpose	Medium	Research uncertainties	Automotive components, industrial applications
Plywood	Mechanical	Reuse, Repurpose, Recover	Low	Degradation from exposure	Construction industry, furniture manufacturing, energy production
Glulam	Mechanical	Reuse, Repurpose, Recover	Low Medium Low	Adhesives complicate separation	Building and construction, energy production
Timber, bamboo	Mechanical	Reuse, Repurpose, Recover	Low	Possible degraded mech. proprieties	Building and construction, consumer industry, energy production
GFRP	Mechanical	Reuse, Repurpose	Low	Possible degraded mech. proprieties Potential for harmful emissions	Construction industry, energy production, energy production
	Thermal, Chemical	Repurpose, Recover	High	High energy consumption	Aerospace, automotive, sports equipment

chemical methods undergo studies to decrease their current energy, technical and cost challenges (Qureshi, 2022).

Neither of the materials preselected for the cut-out application, plywood or NFRP, are typically reused due to outdoor exposure but they have low or medium recycling costs for repurpose. Recycled plywood is not available because it is derived directly from wood logs, but it can be mechanically processed into strands for the production of Oriented Strand Board (OSB) (Nguyen et al., 2023) or reprocessed into thin layers for glue cross-laminated plywood (Nielsen-Roine & Meyboom, 2024). The cost of thermal recycling of NFRP can be lower compared to GFRP due to the possibility of combining the process with thermal reprocessing like compression moulding and injection moulding (Zhao et al., 2022). Note that data on the environmental impact and properties of recycled NFRP is limited. Still, market interest and research are expected to increase due to the rising demand for lightweight composites in the automotive industry (Zhao et al. 2022).

From the collected information and analyses, NFRP and plywood emerged as the strongest candidate for the proposed cut-out bending active design concept. To comprehensively visualize the costs-benefits of the two solutions, Table 5 summarizes the aspects by which the two solutions differ the most and reports the embodied carbon resulting from the temporary and prolonged usage scenarios discussed in the previous Section, for the maximum and minimum densities of the materials. Notice that, in case of NFRP, an embodied carbon of 2 $kgCO_2e/kg$ has been tentatively set, whereas in case of plywood, the material quantities have been calculated considering the whole, gross surface, due to the waste produced by the laser cutting process. It emerges from the table that neither solution is a universal "winner." Plywood is well-

Table 5.
Installation Feasibility comparison-based rating of FPMBSs

CRITERIUM	Plywood	NFRP
Material Ratio (R)	9.09	13.25
Manufacturing challenges	Production of waste	Fiber alignment sensitivity
Embodied Carbon ($kgCO_2$) - temporary usage	869 -1390	1133 to 2124
Embodied Carbon ($kgCO_2$) - permanent usage	1001-1602	1287 to 2413
Erection challenges	Very slow erection process, especially for thick structures; risk of rupture	Succeeded at small scale and large curvature, no available data from architectural projects
Usage challenges	May require maintenance	Humidity, may require protection from agents
Recyclability	Mechanical	Mechanical or chemical (emerging)

established and easily sourced but may require slower bending processes for thicker elements. NFRP offers higher performance and promising sustainability, provided manufacturing quality is rigorously controlled, and end-of-life recycling improves. The more critical path to prototyping and the higher strength suggest however that NFRP may be a promising candidate for active bending structures aimed at prolonged usage, while plywood confirms to be a good solution for temporary structures.

5. CONCLUSION

The bending-active approach represents a form-finding design technique that emphasizes efficiency and innovation across material use, manufacturing, transportation, and construction processes. This method minimizes material waste and reduces the impact of transportation by allowing materials to be deformed on-site directly into their desired forms. Historically, the complexity of designing these structures positioned them primarily as an engineering task, which limited the widespread application in practice. The cut out bending process described in this paper is accessible early in the design phases and paves the way for more integrated and sustainable solutions. This concept utilizes a continuous structure that does not require post-construction joining elements and incorporates a hierarchy of primary and secondary elements. The position and size of these elements can be customized to meet diverse requirements. The paper has discussed how this concept may be implemented considering technological readiness, structural feasibility and environmental sustainability. Preliminary analyses suggest that 3D printing could be a strategy worth exploring, especially for permanent structures, due to its potential for structural and material-level optimization, but suitable composite materials shall be carefully produced for the scope. Laser cut plywood, on the other hand, is a possibility currently closer to implementation and well suited for temporary structures. However, further research is essential to fully realize the practical applications of the design concept.

By examining the interplay between design variables, material choices, construction technologies, and sustainability considerations, the paper has highlighted limitations that need to be addressed in the successive design stages. The preliminary study confirmed that topology and size of the elements are needed within the design rationalization phase for increasing the resistance by form offered by double curvature surfaces, especially under wind load. The connection between the main structural ribs – oriented along principal curvature lines – and the secondary stiffening elements – aligned with geodesic lines – deserves focused study for shape optimization, ensuring adequate strength during use and sufficient deformation during erection. Scalability is a key factor to verify erection challenges because the structural behaviour of larger bending-active systems and may differ from that of small-scale models. Finally, although NFRP has emerged as an interesting opportunity, the many variables within the manufacturing process create uncertainties about its structural and environmental performance, which require focused investigation.

Despite the large amount of work ahead, this paper contributes by highlighting the need for a more holistic approach to the sustainability of bending-active structures and the novel possibilities offered by contemporary manufacturing methods and sustainable material research.

ACKNOWLEDGEMENT

A preliminary version of this paper was presented in the 2024 International Conference on Architecture, Technology, and Innovation (ATI), held on October 3-4, 2024, in Izmir, Turkey.

REFERENCES

[1] Beatini, V. (2017a). Kinetic rosette patterns and tessellations. *International Journal of Computational Methods and Experimental Measurements, 5*(4), 631–641.

[2] Beatini, V. (2017b). Symmetry-based transformable and foldable plate structures. *Journal of Mechanical Design, 139*(7), 072301.

[3] Beatini, V., & Royer-Carfagni, G. (2017). Soap film analogy for anisotropically stretched membranes and cable nets. *Structural and Multidisciplinary Optimization, 55*(3), 885–898. https://doi.org/10.1007/s00158-016-1533-z

[4] Buckminster, F. R. (1959). Self-strutted geodesic plydome (United States Patent No. US2905113A). https://patents.google.com/patent/US2905113A/en

[5] Chauhan, V., Kärki, T., & Varis, J. (2022). Review of natural fiber-reinforced engineering plastic composites, their applications in the transportation sector and processing techniques. *Journal of Thermoplastic Composite Materials, 35*(8), 1169–1209. https://doi.org/10.1177/0892705719889095

[6] Chilton, J., & Tang, G. (2016). Timber gridshells: Architecture, structure and craft. Routledge. https://www.taylorfrancis.com/books/mono/10.4324/9781315773872/timber-gridshells-john-chilton-gabriel-tang

[7] de Grey, S. (2000). The design of the roofs of the British Museum Great Court and the Music Centre at Gateshead. *Widespan Roof Structures*, 276–282.

[8] Douthe, C., Caron, J.-F., & Baverel, O. (2010). Gridshell structures in glass fibre reinforced polymers. *Construction and Building Materials, 24*(9), 1580–1589.

[9] Douthe, C., Mesnil, R., Orts, H., & Baverel, O. (2017). Isoradial meshes: Covering elastic gridshells with planar facets. *Automation in Construction*, 83, 222–236. https://doi.org/10.1016/j.autcon.2017.08.015

[10] Engel, H. (1968). Structure systems. New York, Praeger

[11] Fathollahi A., Beatini V. (2024). Design and analysis of bending-active configurations through an initial flat-cut pattern based on the curvature lines. International Journal of Space Structures.

[12] Gengnagel, C., Hernández, E. L., & Bäumer, R. (2013). Natural-fibre-reinforced plastics in actively bent structures. *Proceedings of the Institution of Civil Engineers - Construction Materials, 166*(6), 365–377. https://doi.org/10.1680/coma.12.00026

[13] Harris, R., Romer, J., Kelly, O., & Johnson, S. (2003). Design and construction of the Downland Gridshell. *Building Research & Information, 31*(6), 427–454. https://doi.org/10.1080/0961321032000088007

[14] Højbjerg, K., Kirkegaard, P. H., & Beatini, V. (2020). Implementation of constructability in conceptual design. 2020(19), 1–13.

[15] Kansara, H., Liu, M., He, Y., & Tan, W. (2023). Inverse design and additive manufacturing of shape-morphing structures based on functionally graded composites. *Journal of the Mechanics and Physics of Solids*, 180, 105382. https://doi.org/10.1016/j.jmps.2023.105382

[16] Khojastehmehr, F., & Filz, G. H. (2023). Expanding the design freedom of spatial patterns by combined elastic bending and twisting: *A parametric study. Proceedings of IASS Annual Symposia, 2023*(26), 1–12. https://www.ingentaconnect.com/contentone/iass/piass/2023/00002023/00000026/art00005

[17] Kotelnikova-Weiler, N., Douthe, C., Hernandez, E. L., Baverel, O., Gengnagel, C., & Caron, J.-F. (2013). Materials for Actively-Bent Structures. *International Journal of Space Structures, 28*(3–4), 229–240. https://doi.org/10.1260/0266-3511.28.3-4.229

[18] Lázaro, C., Monleón, S., & Bessini, J. (2017). Tangent stiffness in point-loaded elastica arches. Proceedings of IASS Annual Symposia, 2017(16), 1–8. https://www.ingentaconnect.com/content/iass/piass/2017/00002017/00000016/art00002

[19] Lienhard, J. (2014). Bending-active structures: Form-finding strategies using elastic deformation in static and kinetic systems and the structural potentials therein.

[20] Liuti, A., Mazzola, C., & Zanelli, A. (2018). Where design meets construction: A review of bending active structures.

[21] Magna, R. L., & Knippers, J. (2017). On the behaviour of bending-active plate structures. *Proceedings of IASS Annual Symposia, 2017*(14), 1–9. https://www.ingentaconnect.com/content/iass/piass/2017/00002017/00000014/art00003

[22] Naicu, D. I. (2012). Geometry and Performance of Timber Gridshells [Master thesis.]. University of Bath.

[23] Nguyen, D. L., Luedtke, J., Nopens, M., & Krause, A. (2023). Production of wood-based panel from recycled wood resource: A literature review. *European Journal of Wood and Wood Products, 81*(3), 557–570. https://doi.org/10.1007/s00107-023-01937-4

[24] Nielsen-Roine, K., & Meyboom, A. (2024). Seven Generationsfor Wood. 12 ACSA Annual Meeting. Disrupters on the Edge.

[25] O'Neill, B. (2006). Elementary differential geometry. Elsevier. https://books.google.ch/books?hl=en&lr=&id=OtbNXAIve_AC&oi=fnd&pg=PP1&dq=O%E2%80%99Neill,+B.,+Elementary+Differential+Geometry&ots=aNHm7RJIEn&sig=6fT4nPxUNIrYDLzwbcXqcAhOG3c

[26] Oun, A., Alajarmeh, O., Manalo, A., Abousnina, R., & Gerdes, A. (2024). Durability of hybrid flax fibre-reinforced epoxy composites with graphene in hygrothermal environment. *Construction and Building Materials*, 420, 135584. https://doi.org/10.1016/j.conbuildmat.2024.135584

[27] Quinn, G., & Gengnagel, C. (2015). Simulation Methods for the Erection of Strained Grid Shells Via Pneumatic Falsework. https://doi.org/10.1007/978-3-319-24208-8_22

[28] Qureshi, J. (2022). A review of recycling methods for fibre reinforced polymer composites. *Sustainability, 14*(24), 16855.

[29] Radeschi, M. (2017). Closed geodesics on surfaces and Riemannian manifolds. 5. https://doi.org/10.14760/SNAP-2017-005-EN

[30] Saslawsky, K., Steixner, C., Tucker, M., Costalonga, V., & Dahy, H. (2024). FlaxPack: Tailored Natural Fiber Reinforced (NFRP) *Compliant Folding Corrugation for Reversibly Deployable Bending-Active Curved Structures. Polymers, 16*(4), 515. https://doi.org/10.3390/polym16040515

[31] Schling, E., Wang, H., Hoyer, S., & Pottmann, H. (2022). Designing Asymptotic Geodesic Hybrid Gridshells. *Computer-Aided Design*, 152, 103378. https://doi.org/10.1016/j.cad.2022.103378

[32] Schmucker, D. G. (1998). Models, Models, Models: The Use Of Physical Models To Enhance The Structural Engineering Experience. 1998 Annual Conference, 3–413.

[33] Tellier, X., Boutillier, R., Douthe, C., & Baverel, O. (2021). Patterns for gridshells with negligible geometrical torsion at nodes. *Curved and Layered Structures, 8*(1), 147–156.

[34] Tuli, N. T., Khatun, S., & Rashid, A. B. (2024). Unlocking the future of precision manufacturing: A comprehensive exploration of 3D printing with fiber-reinforced composites in aerospace, automotive, medical, and consumer industries. *Heliyon, 10*(5), e27328. https://doi.org/10.1016/j.heliyon.2024.e27328

[35] Wang, T., Wang, Y., Crocetti, R., & Wålinder, M. (2022). In-plane mechanical properties of birch plywood. *Construction and Building Materials*, 340, 127852. https://doi.org/10.1016/j.conbuildmat.2022.127852

[36] Wei, Y., & Hadigheh, S. A. (2022). Cost benefit and life cycle analysis of CFRP and GFRP waste treatment methods. *Construction and Building Materials*, 348, 128654.

[37] Young, W. C., Budynas, R. G., & Sadegh, A. M. (2002). Roark's formulas for stress and strain (Vol. 7). McGraw-hill New York. https://jackson.engr.tamu.edu/wp-content/uploads/sites/229/2023/03/Roarks-formulas-for-stress-and-strain.pdf

[38] Zhang, Y., Yan, Z., Nan, K., Xiao, D., Liu, Y., Luan, H., Fu, H., Wang, X., Yang, Q., Wang, J., Ren, W., Si, H., Liu, F., Yang, L., Li, H., Wang, J., Guo, X., Luo, H., Wang, L., … Rogers, J. A. (2015). A mechanically driven form of Kirigami as a route to 3D mesostructures in micro/nanomembranes. *Proceedings of the National Academy of Sciences, 112*(38), 11757–11764. https://doi.org/10.1073/pnas.1515602112

[39] Zhao, X., Copenhaver, K., Wang, L., Korey, M., Gardner, D. J., Li, K., Lamm, M. E., Kishore, V., Bhagia, S., & Tajvidi, M. (2022). Recycling of natural fiber composites: Challenges and opportunities. Resources, *Conservation and Recycling*, 177, 105962.